

AIRPHANT: Cloud-oriented Document Indexing

Supawit Chockchowwat, Chaitanya Sood and Yongjoo Park
University of Illinois at Urbana-Champaign
{supawit2,csood2,yongjoo}@illinois.edu

Abstract—Modern data warehouses can scale compute nodes independently of storage. These systems persist their data on cloud storage, which is always available and cost-efficient. Ad-hoc compute nodes then fetch necessary data on-demand from cloud storage. This ability to quickly scale or shrink data systems is highly beneficial if query workloads may change over time.

We apply this new architecture to *search engines* with a focus on optimizing their latencies in cloud environments. However, simply placing existing search engines (e.g., Apache Lucene) on top of cloud storage significantly increases their end-to-end query latencies (i.e., more than 6 seconds on average in one of our studies). This is because their indexes can incur multiple network round-trips due to their hierarchical structure (e.g., skip lists, B-trees, learned indexes). To address this issue, we develop a new statistical index (called IoU Sketch). For lookup, IoU Sketch makes multiple asynchronous network requests in parallel. While IoU Sketch may fetch more bytes than existing indexes, it significantly reduces the index lookup time because parallel requests do not block each other. Based on IoU Sketch, we build an end-to-end search engine, called AIRPHANT; we describe how AIRPHANT builds, optimizes, and manages IoU Sketch; and ultimately, supports keyword-based querying. In our experiments with four real datasets, AIRPHANT’s average end-to-end latencies are between 13 milliseconds and 300 milliseconds, being up to $8.97\times$ faster than Apache Lucene and $113.39\times$ faster than Elasticsearch.

I. INTRODUCTION

In public clouds, compute and storage can be scaled independently. Based on this, modern data warehouses including Snowflake [1], Google BigQuery [2], Amazon Redshift [3], and Presto [4], [5] allow users to quickly start new clusters, analyze a large volume of data retrieved on demand from cloud storage (e.g., AWS S3 [6], Azure Blob Storage [7], GCP Cloud Storage [8]), and finally terminate those clusters if they are no longer needed.¹ Users can easily tune many properties of those clusters such as number of nodes, number of cores, memory size. To maximize the performance, users can upgrade their clusters. To reduce the cost, users can downsize their clusters. Users can thus fine-tune the overall cluster bill and expected performance; regardless, their data is kept independently in cloud storage, offering cost-efficiency and robustness.² This capability to quickly scale up and down clusters has been well

received.³ We refer to this new architectural shift as *separation of compute and storage*.

a) New Direction: We investigate applying this new architectural shift to *search engines*. Search engines are systems for retrieving relevant documents that contain user-provided search keywords. Commonly used search engines all rely on some form of indexes (e.g., skip lists [11], B+ tree [12]–[14], learned indexes [15], [16]) to quickly find relevant documents. For fast index traversals, they need their compute and storage closely located on the same machine. This architecture has a disadvantage that we need to keep a large cluster running as more documents are indexed, even if query workloads are light or even if some documents are queried infrequently.

However, if we can build a special index stored entirely in cloud storage, we can scale compute nodes independently of indexing. This offers flexibility when query workloads change over time or inquire about particular documents more frequently than others. For instance, rarely queried documents can simply be dormant in low-cost cloud storage along with their index. This new approach, if possible, can enable highly cost-efficient searching.

b) Challenges: Existing search engines do not perform well under the separation of compute and storage. Because existing indexes have hierarchical structures [11]–[17], they incur significant traversal overhead when the data is moved further away from compute. To identify *postings* (i.e. references to documents) of documents that contain the search keywords, or specifically, to locate the data block containing those postings (called a *postings list*), an existing index requires traversing from its root, to a child node at the next level, and so on, until we reach a leaf node. In this process, to go one level deeper, we need to fetch the next node from the storage device, incurring an additional communication. This means that to reach a leaf node at level N , we need to make N sequential back-to-back communications. If those individual communications are fast enough (e.g., local SSDs), the end-to-end latency for N communications may be tolerable. However, if those nodes are stored in cloud storage, each communication needs a network round-trip, which can be orders of magnitude slower than local SSDs. If such communications must be made sequentially multiple times, the total end-to-end latency quickly adds up, significantly affecting end-user experiences. Although node caching

¹Google BigQuery effectively takes this series of operations. However, they are hidden from users’ perspective; the users are charged based on the cost of each query.

²Note that compute resources (e.g., cores, memory) typically takes a larger portion in cloud bills than storage. Thus, scaling down compute nodes can lead to bigger savings.

³For example, as of early 2021, Snowflake is one of the fastest growing private companies in the data space, with its market capitalization reaching about \$70 billion [9]. Also, Amazon Redshift introduced in December 2019 a new type of node called `ra3`, which offers the flexibility in adjusting cluster sizes [10].

may reduce communications, allocating a large enough cache to store the entire index is prohibitively expensive when the corpus size is large. For this reason, it is generally hard to avoid multiple sequential communications in existing indexes. On a separate note, Elasticsearch has a S3 plugin, only for snapshots [18], but not for interactive querying.

c) Our System: We introduce AIRPHANT,⁴ a new search engine specifically designed for low-latency querying under the separation of compute and storage. While AIRPHANT requires several nontraditional design decisions, its core idea is straightforward: *to minimize end-to-end query latencies, we should completely avoid sequential back-to-back communications with cloud storage.* Instead, AIRPHANT issues multiple asynchronous requests in parallel (thus, no blocking in between) to obtain a *postings list*. This asynchronous approach is enabled by our novel statistical index. Once we have a postings list, the rest of the process is almost identical; AIRPHANT retrieves individual documents and presents them to users.

As noted above, the crux of AIRPHANT is our statistical index called *Intersection of Unions Sketch (IoU Sketch)* (§VI-B). Unlike existing index structures, IoU Sketch initially produces multiple *super postings lists (superpost)*, where each superpost contains both: 1) all relevant postings of documents containing search keywords, and 2) some irrelevant postings of the documents not containing search keywords. These superposts have two important properties. First, they are independent from each other in retrieval process; thus, we can retrieve them in parallel. Second, by intersecting them, the number of irrelevant documents reduces exponentially due to their incoherence enforced by randomization. Thus, the final postings list—the intersection of all superposts—is *almost* identical to the one from existing indexes.

Yet the final postings list may contain a few false positives in expectation. Nonetheless, AIRPHANT removes them as it retrieves actual content of documents at a later step, recovering a perfect precision as a result. Also importantly, superposts and so the final postings list contain no false negative; AIRPHANT recalls all documents that indeed contain search keywords. Moreover, IoU Sketch is carefully optimized according to a word frequency distribution in the corpus and queries (§VI-B) given memory and accuracy constraints. Although these false positives lead to an additional cost in document retrieval, IoU Sketch’s performance benefit overcomes such cost, leading to an improvement over existing indexing techniques. As a result, AIRPHANT significantly outperforms existing search engines deployed similarly, keeping its query latencies always under a second even for the largest dataset we have tested. IoU Sketch is built per corpus; thus, it is sufficient to download it only once before querying. In addition, its size is configurable (less than 2MB in our experiments), making IoU Sketch lightweight to keep it in memory.

d) Summary of Contributions: The contributions of this work are organized as follows:

1. We introduce AIRPHANT, a new search engine optimized for cloud environments. Following the separation of compute and storage, AIRPHANT persists all data (indexes and documents) in cloud storage. (§II and §III)
2. We describe a novel statistical index called IoU Sketch as a core component of AIRPHANT. IoU Sketch can accurately identify documents containing search keywords with a single batch of concurrent communications with cloud storage; consequently, its end-to-end latency is significantly shorter than existing indexes. (§IV)
3. We show how we can optimize IoU Sketch for a given corpus and requirement. Specifically, we express IoU Sketch’s accuracy in terms of expected number of false positives parameterized by IoU Sketch structure. Then, we analyze and present an efficient optimization algorithm. (§IV)
4. We empirically compare and analyze the performance of AIRPHANT to other existing systems such as Lucene [19], Elasticsearch [20], SQLite [21], and naïve hash table. (§V)

II. AIRPHANT: CORE IDEAS

This section introduces the core ideas of AIRPHANT. For this, we first briefly recap core concepts in search engines (§II-A). Next, we discuss system challenges of running search engines on top of cloud storage (§II-B). Finally, we present the core ideas of AIRPHANT for addressing those challenges (§II-C).

A. Search Engines: Background

This section overviews the core concepts in document indexing and searching [22]. First, we describe high-level user interface of search engines. Next, we describe how a search engine quickly finds the documents containing a search keyword.

a) User Interface: We briefly describe a typical programming interface of search engines from end users’ perspectives. Figure 1 shows an example code snippet for creating/indexing documents and performing a keyword-based search. The strings passed to document objects (i.e., "hello world" and "hello airphant") are parsed by the search engine into multiple words (i.e., "hello" and "world" for doc1; "hello" and "airphant" for doc2). These parsing rules are configurable by users [23]. Then, the user can use any of those parsed keywords (i.e., hello, world, airphant) for searching.

b) Internal Workflow: A typical search engine internally implements an inverted index to retrieve relevant documents. An inverted index is a data structure to quickly identify the documents containing a search keyword. It normally consists of two sub-components: 1) *postings lists*, and 2) *term index*. A postings list is a list of document IDs (e.g., doc1 and doc2) containing an associated keyword (e.g., "hello"). There are as many postings lists as the number of indexed keywords. The term index is a map from each keyword (e.g., "hello") to the location of its associated postings list. For fast searching, the term index should be able to quickly return the location of the postings list. B-trees and skip lists and commonly used

⁴A portmanteau from "air" and "elephant", signifying the lightweight system capable of serving from a large corpus

```

// index two documents
Index index = new Index();
Document doc1 = new Document("hello world");
index.addDocument(doc1);
Document doc2 = new Document("hello airphant");
index.addDocument(doc2);

// search for documents containing "airphant"
Document[] docs = index.search("airphant");

```

Fig. 1: Example user interface of a search engine

data structures for their asymptotically fast lookup operations. Inverted indexes (both postings lists and term index) are constructed when documents are inserted into a search engine.

Given a query keyword, a search engine performs the following operations. First, using the term index, it identifies the location of the postings list associated with the search keyword. Second, it fetches the postings list for the search keyword. Third, it fetches the actual contents of the documents and return them to the user.

For the term index, hierarchical indexes are commonly used. A skip list [11], [24] is used by Apache Lucene [19], an underlying engine for distributed search engines such as Elasticsearch [20] and Apache Solr [25]. While it is probabilistic, a skip list needs $O(\log n)$ steps on average for each lookup. A B-tree can also be used for the term index, which has the same lookup cost $O(\log n)$.

B. Search Engines on Cloud: Challenges

Placing search engines directly on top of cloud storage increases their end-to-end search latencies significantly. One critical performance bottleneck comes from term indexes. We first explain why a term index lookup operations slow down substantially. Then, we describe why simple alternative approaches are not likely to solve the issue. These challenges motivate AIRPHANT (§II-C).

a) Cloud Storage: Major public cloud computing vendors (e.g., AWS, GCP, Azure) all offer cloud storage services. Simply speaking, these services are object storage where each object or *blob* is identified by a name. To upload and download data to and from cloud storage, vendor-provided programming APIs are used. These APIs make requests over the network to fetch data. These services are robust against data loss (e.g., 99.999999999% durability of AWS S3) and cost-efficient (\$20/TB/month at the time of writing).

b) Performance Challenge: While the network bandwidth is increasing, we observe that *network latency*—the time to get the first byte—acts as a critical bottleneck for search engines. That is, whether we are retrieving a smaller or larger volume of data, there is some overhead we must pay for every network request. This network latency causes an affine relationship between 1) the size of data to fetch and 2) the total elapsed time (referred to as *retrieval latency*). Figure 2 depicts such a relationship using a small virtual machine (2 cores, 2GB memory) with multithreaded download on Google Cloud Note that both X-axis and Y-axis are in log-scale. The figure shows that the retrieval latency remains around 50 milliseconds until

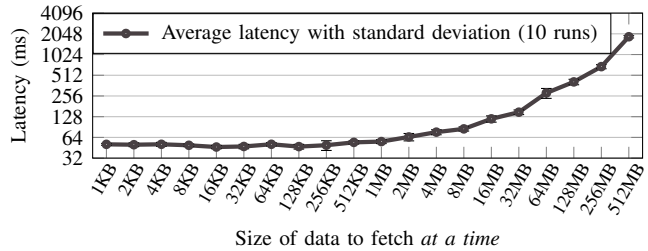


Fig. 2: End-to-end latency between Google Cloud virtual machines and Google Cloud Storage.

we increase the data size beyond 2MB. After that point, the retrieval latency increases linearly.

This affine characteristic of network performance causes existing search engines to perform poorly. To find the postings list for a keyword, a search engine performs a lookup using a term index. This lookup may involve multiple round-trips to storage devices for fetching intermediate nodes.⁵ If the storage device is cloud storage (not a local SSD), each round-trip incurs a network latency. When multiple network requests are made, lookup latency quickly increases even if each trip retrieves a small amount of data. Parallelizing these network requests is non-trivial because in order to make the *next* network request, we need the information obtained from the *previous* network request. Of course, if we can cache the entire term indexes in memory for every corpus, we can completely avoid any communications over the network. However, such scenario requires expensive equipment and so the approach is costly. As described in §I, our goal is the opposite: we want to minimize our compute resources without much sacrificing search performance.

C. Statistical Approach to Indexing

In this section, we present the core ideas of our statistical indexing. Its primary goal is to avoid multiple sequential communications in obtaining a postings list. To achieve this, we propose non-trivial changes to inverted indexes. In essence, it makes the following systems tradeoff: the payloads of individual requests become larger, but those requests are made in parallel.

a) Bins: To keep the pointers to *all* postings lists in memory, we form *bins* by merging multiple keywords. Accordingly, associated postings lists are also merged into one. For example, consider three regular keywords and their postings lists: (“hello” → (doc1, doc2)), (“world” → (doc1)), and (“airphant” → (doc2, doc3)). Suppose we merge “hello” and “world” into one bin b_1 , which produces: (b_1 → (doc1, doc2)), (“airphant” → (doc2, doc3)). After merge, the number of keywords is reduced from three to two, but we no longer have exact postings list for merged keywords. In other words, the postings list for b_1 contain both the postings list for “hello” and the list for “world”. Thus, some of the documents in (doc1, doc2) may not contain “hello” (false positives); however, no other documents contain “hello” (*no false negatives*). Systematically,

⁵See our description on term index operations in §II-A.

we rely on hash functions to determine how to group original keywords into bins.

This merge operation has one drawback: we will have to fetch more documents. This drawback is more significant if there are much fewer bins than original keywords (e.g., 1000 keywords to 1 bin on average). Note that although the false positive documents can be removed by examining the actual content, in order to do so, we must first fetch those documents. Fetching, say, $1000\times$ more documents can slow down end-to-end search latencies greatly. To address this, we exploit the probabilistic nature of random merge, as described below.

b) Multi-layer Structure: Retrieving a large number of actual documents is slow. To avoid this, we reduce false positives by extending the above approach. Note that merging keywords produces a map from a bin to a (merged) postings list. By repeating this merge operation, we construct a multi-layer (say L layers) structure where each layer contains a different hash function. Different hash functions produce different groupings; thus, each layer is associated with different sets of bins.

Given a keyword, we use this L -layer structure to obtain an accurate postings list, as follows. First, we apply L hash functions to a keyword, and look up those hash values in our multi-layer maps; then, we obtain the *pointers* to L postings lists. Second, we fetch L postings lists in parallel from cloud storage (here, we make a single batch of concurrent network requests). Finally, we intersect those L postings lists to obtain a final posting list.

The final postings list is accurate (i.e., small false positives) because most false positives are eliminated as part of intersection operations. This is due to *the multiplication rule for independent events* in probability. That is, if we consider a single merge operation, it introduces many false positives into a postings list (from the perspective of one of the merged keywords). However, if we consider multiple independent merge operations and take only the common postings among them, the number of false positives decreases exponentially. We formally discuss its mathematical properties in §IV. The multi-layer structure is still memory-efficient because it only stores hash functions and the pointers to (merged) postings lists; it does not store original keywords.

III. SYSTEM DESIGN

We describe AIRPHANT’s core building blocks and concepts, with a focus on their high-level operations. Specifically, we present the current scope of AIRPHANT (§III-A), its internal components, and offline operations (e.g., indexing building).

A. Current Scope

AIRPHANT supports important use cases, but its capability is still limited compared to full-fledged search engines such as Elasticsearch [20] and Apache Solr [25]. This section describes what AIRPHANT currently supports: (a) the query workloads it can handle and (b) a few requirements it needs from cloud storage.

TABLE I: Component-wise correspondence between Apache Lucene [19] and AIRPHANT (this work). Skip list and postings list are sub-components of Lucene index. Likewise, MHT and superpost are sub-components of IoU Sketch.

| Apache Lucene | AIRPHANT (Ours) |
|-------------------------------|-----------------------------------|
| Lucene index (inverted index) | IoU Sketch |
| · Skip Lists (term index) | · Multilayer Hash Table (MHT) |
| · Postings List | · Super Postings List (superpost) |

a) Documents and Queries: AIRPHANT offers document searches with exact keyword matching; that is, it finds the documents containing a given set of keywords. In comparison, existing full-fledged search engines also support others such as range queries, fuzzy queries, etc. AIRPHANT aims towards read-oriented workloads where the corpus doesn’t change frequently. This focus allows many design decisions to fully harness strength of cloud storage. As of now, extensions to support a wider class of queries and handle frequent corpus updates are deferred to future works.

b) Target Environments: AIRPHANT targets modern public cloud, where compute nodes can quickly turn on and off while most data can be stored safely in cloud storage. AIRPHANT heavily relies on cloud storage for data management. It indexes the documents stored in cloud storage and subsequently persists index structures in cloud storage as well. It assumes that cloud storage offers random read operations; that is, fetching bytes from an arbitrary offset doesn’t require full read. Random reads are useful in packing multiple postings lists in a single blob; AIRPHANT can read arbitrary postings lists without performance penalty. Also, keeping all postings lists in a few blob makes the overall data management easier because otherwise, we will need as many blobs as the number of bins. Random reads are already supported by major cloud vendors [26]–[28]. Note that original documents may be stored in a single blob (e.g., delimited by line breaks) or in different blobs. In each posting, AIRPHANT records (blob name, offset, length) as part of a document identifier.

After constructing necessary structures, AIRPHANT Searcher (described later shortly) can reside anywhere with an access to the cloud storage to serve search queries. Because of its configurable memory usage, it can be sufficiently portable to deploy on IoT and mobile devices, or it can inflate to support a humongous corpus on powerful machines. Perhaps one of interesting settings is the serverless deployment serving query requests, for example, function-as-a-service (FaaS) e.g. Google Cloud Functions [29], AWS Lambda [30], and Microsoft Azure Functions [31]. Because of the minimal initialization, the deployment manager can quickly scale up or down based on the current demand across different corpuses.

B. Statistical Inverted Index

This section describes systems aspect of our statistical (inverted) index. We will mention core concepts introduced

in §II-C, with a focus on deployment and management perspectives.

Our statistical index is called *IoU Sketch*; we named it IoU or *intersection of unions* because our index construction involves unioning (or merging) multiple postings lists into one, and our search involves intersecting multiple postings lists. IoU Sketch consists of two sub-components: a multi-layer hash table (MHT) and super postings lists (superposts). MHT is the multi-layer map we described in §II-C. Superposts are merged postings lists (also described in §II-C). MHT is downloaded and kept in memory when a certain corpus is searched for the first time. Superposts are always kept on cloud storage. To clarify their roles in existing contexts, Table I makes one-to-one comparisons between Apache Lucene and ours. Of course, their internal operations are different.

C. Components and Workflow

AIRPHANT consists of two components: Builder and Searcher. Builder creates and persists an index; Searchers uses the index for querying.

a) Builder Workflow: AIRPHANT Builder (or simply, Builder) is a component that creates IoU Sketchs and persists them on cloud storage. Builder creates a single IoU sketch per corpus. Each IoU Sketch consists of superposts and MHT, both of which Builder creates and persists. Figure 3 lays out the steps to build IoU Sketch from profiling to optimization.

Builder’s index creation starts when the user passes a corpus and configurations. Builder uses a corpus-document parser to unwrap a blob into documents and generate postings that refer to their documents’ byte ranges, allowing direct retrieval afterwards. Builder then uses a document-word parser to extract words. The user can select both a corpus-document and a document-word parsers for each corpus. By default, a single blob may contain multiple documents; however, developers can override this with custom parsers.

These parsed documents are then profiled to collect statistics necessary for index building. AIRPHANT Builder makes a single pass over all documents during profiling. The collected statistics include the total numbers of documents and words, document lengths, and document frequencies (i.e., the number of documents that contains a specific word). The statistics are used for IoU’s structural optimization (§§ IV-A and IV-E).

Based on the profile, Builder optimizes its IoU Sketch structure using the algorithm described in §IV-A. The accuracy and memory requirements may also be specified. Alternative to auto-tuning, users can also manually select the IoU Sketch structure, skipping both profiling and optimization steps.

Builder first creates superposts. AIRPHANT Builder generates superposts from all documents. That is, a superpost is constructed for each bin, and a collection of all superposts are persisted. Recall that each superpost is a list of merged postings, where each posting comprises (a blob name, an offset, and a length), which are used to locate actual documents. The collection of superposts are concatenated into a single blob using a compaction encoding (§IV-C). This makes data management easier.

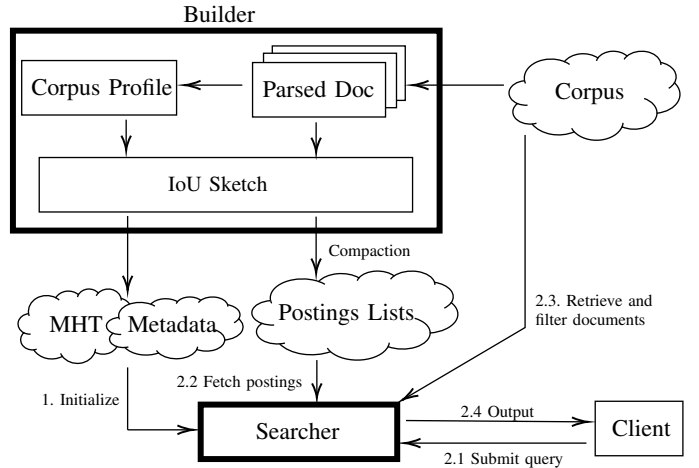


Fig. 3: AIRPHANT Overview

Next, Builder creates a MHT. MHT stores the pointers to those superposts, which are compacted in a single blob. To locate each superpoint, MHT’s pointer has a blob name, byte offset, and byte size. In addition, Builder stores seeds of hash functions (used for creating super posts) and other metadata in the same file. This file is persisted as another blob.

b) Configuring Builder: The user can configure AIRPHANT in different ways. A storage driver specifies how to read a corpus. Parsers specifies how to separate documents in a corpus and how to extract keywords from a document. The accuracy of IoU sketch can be set in terms of average number of irrelevant documents (i.e, false positive rate). The memory limit on MHT can also be placed.

c) Searcher: AIRPHANT Searcher (or simply, Searcher) is a light-weight component that retrieves the documents containing search keywords. Searcher relies on IoU Sketches. Searcher performs two types of operations: initialization and querying. Initialization happens only once per corpus. Querying happens for each query. The same diagram (Figure 3) illustrates the two procedures to fulfill queries: initialization and querying.

When a user opens a corpus, Searcher initializes itself from cloud-stored index structure; it retrieves hash seeds and postings list pointers (for MHT), both of whose memory footprint is predictable and controllable via IoU Sketch configuration. It then reconstructs hash functions, and hence, MHT.

When a query arrives, Searcher hashes each word in the query to collect a set of pointers to postings list. Using these pointers, Searcher concurrently fetches the corresponding postings lists from cloud storage and computes the intersection of postings lists (i.e., the final postings list). This is the only batch of concurrent requests for lookup. Then, the documents identified by this final postings list is retrieved from cloud storage. Finally, Searcher filters out irrelevant documents after fetching the documents. This filtering process is much fast compared to document-fetching. The user can also fetch only top K relevant documents, which is useful for lowering latencies (§IV-D).

IV. STATISTICAL INVERTED INDEX

In this section, we detail our statistical inverted index (IoU Sketch). First, we define IoU Sketch (§IV-A). Then, we detail corpus profiling (§IV-B) and superposts encoding (§IV-C). Next, we introduce two techniques to accelerate AIRPHANT query: top- K queries (§IV-D) and special handling of extremely common words (§IV-E).

A. IoU Sketch

IoU Sketch is the core index data structure that maps a keyword to a postings list. We first explain its data structure and interface as well as raw parameters. Second, given a corpus, we analyze the expected accuracy based on specific settings of raw parameters. Because one of raw parameters is not intuitive from user’s perspective, IoU Sketch offers an alternative configuration based on memory constraint and desired accuracy. Using earlier analysis, it then automatically tunes its raw parameters to meet those constraints and optimize for search performance. Lastly, we further examine tightness of IoU Sketch’s accuracy.

a) *Data Structure*: Internally, IoU Sketch is a L -layer hash table with L different hash functions. Each bin in a table contains a superposts that is aggregated via insertion operations. Under IoU Sketch’s hash functions, any given word is mapped to one bin per layer (L bins in total) where the postings list of the word is guaranteed to be a subset of the superpost in each associated bin. Such guarantee eliminates false negative but entails false positive. IoU Sketch supports two main functionalities.

1. `insert(word, document list)`: For each layer, it hashes the word to find its bin and update bin’s superpost to its union with word’s postings list.
2. `query(word)`: It retrieves superposts from all layers; then, outputs the intersection of all superposts.

For illustration, Figure 4 shows IoU Sketch hash tables after inserting four words w_1 , w_2 , w_3 , and w_4 with different postings lists. Specifically, word w_2 is mapped to (layer1, bin2), (layer2, bin2), and (layer3, bin1) using hash functions from the three layers. It shares the same bin as w_3 in the first layer, w_4 in the second layer, and both w_1 and w_3 in the third layer. Each bin then stores the aggregated superpost of the words; for example, the superpost of (layer1, bin2) is the union of postings lists of words w_2 and w_3 : $\{d_2, d_3\} \cup \{d_2, d_3, d_4\} = \{d_2, d_3, d_4\}$. Querying the word w_2 therefore results in a postings list $\{d_2, d_3, d_4\} \cap \{d_2, d_3, d_4, d_5\} \cap \{d_1, d_2, d_3, d_4\} = \{d_2, d_3, d_4\}$ which contains a false positive postings, d_4 . On the other hand, querying the word w_1 fortunately produces in the exact postings list $\{d_1\}$ despite the word sharing bins in second and third layers with other three words.

Recall there are n documents and let B be the total number of bins across all layers. To persist, IoU Sketch only requires superposts and hash seeds to reconstruct itself, making its worst case storage complexity $O(\min\{nmL, Bn + L\})$ if documents have m words on average. To achieve single-cycle retrievals, AIRPHANT Builder split IoU Sketch into superposts

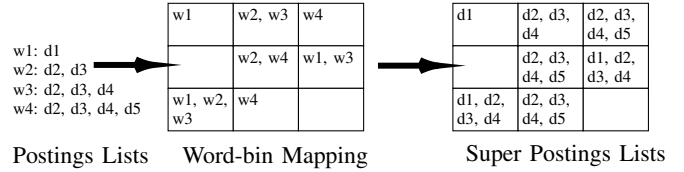


Fig. 4: Example of IoU Sketch for a corpus with 5 documents and 4 distinct words. Word-bin mapping shows sets of words in corresponding IoU Sketch’s bins. Super postings lists are the merged postings lists for those sets of words.

and MHT. It then stores superposts on cloud storage, so that MHT is L layers of hash tables where each entry has a pointer to the corresponding superpost. Therefore, AIRPHANT Searcher needs to hold $O(B)$ of memory for MHT ($O(L)$ hash seeds and $O(B)$ bin pointers where $L \ll B$).

Figure 5 empirically demonstrates that IoU Sketch achieves significantly fewer false positives compared to a hash table ($L = 1$) when B is fixed. As L increases from 1, the number of false positives decreases rapidly. After a certain value, the allocated bins are divided into too many layers, resulting in a smaller number of bins per layer, and consequently, a higher selectivity and more false positives. Not only do these observations justify the use of multiple hash tables over a single one, but it also suggests that there is an optimal choice of L depending on both the corpus and the choice of B .

b) *Expected False Positives*: For a family of pairwise independent hash functions, IoU Sketch selects $(h_l)_{l=1}^L$ where each h_l is the hash function for l -th layer. Let W_i be the set of distinct words in i -th document with its size being $|W_i|$, and W be the set of all words. Suppose B is given and assume B is divisible by L for simplicity, the probability that i -th document is a false positive in a query of any irrelevant word w is $q_i(L) = q_i(L; B, \{W_i\}_{i=1}^n)$. Independence between w and q_i is a result of pairwise independent hash family. Equation (1) also shows the approximation $\hat{q}_i(L)$ whose properties leads to an efficient optimization.

$$q_i(L) = \left[1 - \left(1 - \frac{1}{B/L} \right)^{|W_i|} \right]^L \approx \left[1 - e^{-\frac{|W_i|L}{B}} \right]^L = \hat{q}_i(L) \quad (1)$$

Assume a query word distribution $w \sim \text{Cat}(W, \vec{p})$ where p_w is the prior probability of the word w in a query, Equation (2) describes the expected number of false positives over all words whose unit is count per query. This is the primary objective function to tune IoU Sketch. For brevity, we write $F(L) = F(L; B, \{W_i\}_{i=1}^n)$ and define its approximation $\hat{F}(L)$ similarly using $\hat{q}_i(L)$ in place of $q_i(L)$. Here $c_i = \sum_{w \in W \setminus W_i} p_w$ is the probability of words not contained in i -th document and acts as a linear combination coefficient in F . Figure 5 asserts the resemblance between this formula and empirical observations. In fact, later, we confirms that the observed number of false positives is highly concentrated around this expectation.

$$F(L) = \sum_{i=1}^n \sum_{w \in W \setminus W_i} p_w q_i(L) = \sum_{i=1}^n c_i q_i(L) \quad (2)$$

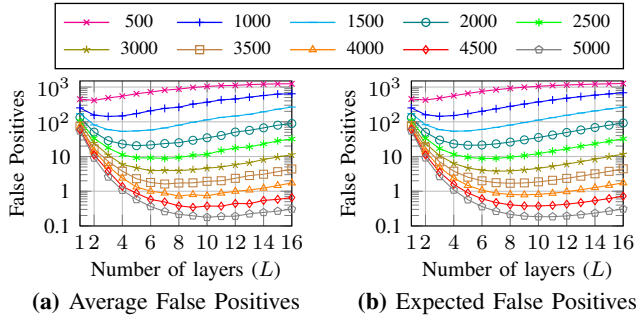


Fig. 5: Average and expected numbers of false positives (count per query) when varying the numbers of layers L and bins B on Cranfield. Each line corresponds each B value.

Even though L is a discrete variable, we extend its domain to a continuous one $L \in \mathbb{R}, 1 \leq L \leq B$ to study richer characteristics of $F(L)$. In particular, the extension endows us with the derivative $\hat{f}(L) = \frac{d}{dL} \hat{F}(L) = \sum_{i=1}^n c_i \hat{q}_i(L)$. We condense the formula by substituting in $z_i(L) = 1 - \exp(-|W_i|L/B)$. The shift of focus towards the approximation eases the analysis and leads to an efficient algorithm to optimize IoU Sketch structure.

$$\hat{q}'_i(L) = z_i(L)^{L-1} [z_i(L) \ln z_i(L) - (1 - z_i(L)) \ln(1 - z_i(L))] \quad (3)$$

c) *Optimization on Number of Layers:* The overall performance improves when the number of layers is smaller since a query would fetch and intersect a fewer superposts. In addition, a larger number of bins would replicate more postings across layers, further increasing the index storage size. Consequently, we are interested in minimizing the number of layers given constraints on the number of bins B and false positives F_0 . In other words, the optimization problem (Equation (4)) finds the smallest number of layers that the (B, L) IoU Sketch has a fewer expected number of false positives than F_0 .

$$L^* = \min L \quad \text{s.t. } 1 \leq L \leq B, F(L; B, \{W_i\}_{i=1}^n) \leq F_0 \quad (4)$$

Unfortunately, $F(L)$ is non-convex and can contain multiple minimizers. Nevertheless, an analysis on its approximation $\hat{F}(L)$ reveals three important characteristics as the building blocks for Algorithm 1. First, there is a region of fast optimization covering practical F_0 values (Lemma 2). Secondly, although L can be as large as B , we only need to search in a much smaller interval (Lemma 3). Finally, there is a relatively cheap lower bound which allows us to quickly check the feasibility (Lemma 1).

With these lemmas in mind, Algorithm 1 first validates the proposed constraints B and F_0 with the lower bound. It then determines whether L falls in the fast or slow region and picks the optimization routine accordingly. For the fast region where $\hat{F}(L)$ is decreasing, it performs a binary search to find the smallest L in the range $[1, L_{\min}]$. On the other hand, the slow region in the range $[L_{\min}, L_{\max}]$ does not guarantee such monotonicity, so the algorithm iteratively attempts increasing

Algorithm 1: Number of Layers Minimization

Input: Number of bins B , expected false positive F_0 , sets of all distinct words $\{W_i\}_{i=1}^n$, query word distribution $\text{Cat}(W, \vec{p})$
Output: Minimum number of layer L^* or rejection

- 1 if $\sum_{i=1}^n c_i 2^{-L_i^*} \leq F_0$ then
- 2 if $\hat{F}(L_{\min}) \leq F_0$ then
- 3 $L^* \leftarrow$ binary search $L \in [1, L_{\min}]$
- 4 else if iterative search $L \in [L_{\min}, L_{\max}]$ succeeds then
- 5 $L^* \leftarrow$ the result from iterative search
- 6 return L^* if assigned, otherwise reject

values of L until the constraint is met. If either the lower bound checking or iterative search fails, it is impossible to find a L that satisfies the constraints and so the algorithm rejects.

Lemma 1. $L_i^* = \arg \min_L \hat{q}_i(L) = \frac{B}{|W_i|} \ln 2$. It immediately follows that $\hat{q}_i(L_i^*) = 2^{-L_i^*}$ and so $\hat{F}(L) \geq \sum_{i=1}^n c_i 2^{-L_i^*}$.

Proof. From Equation (3), the minimizer L_i^* satisfies $\hat{q}'_i(L_i^*) = 0$. Note that the left factor is always positive, so it must be the case that the right factor is zero or equivalently $z_i(L_i^*) = 1/2$. Therefore, $\exp(-|W_i|L_i^*/B) = 1/2$; in other words, $L_i^* = \frac{B}{|W_i|} \ln 2$. Substitute this minimizer to Equation (1) and Equation (2) to produce the two results later. \square

Remark. Because $F(L) > \hat{F}(L)$ for $1 \leq L \leq B$, we have also derived a lower bound $F(L) > \sum_{i=1}^n c_i 2^{-L_i^*}$, validating the feasibility check in alg. 1.

Lemma 2. For $L < \min_i L_i^* = L_{\min}$, expected false positive is strictly and exponentially decreasing $\hat{f}(L) < 0$ and $\hat{F}(L) = O\left(\frac{n}{2L}\right)$.

Proof. Notice that if $L < L_i^*$, $z_i(L) < 1/2$. Using Equation (3), we prove the strictly decreasing property: $\hat{q}'_i(L) < 2^{-L-1} \ln \frac{z_i(L)}{1-z_i(L)} < 0$. Similarly from $z_i(L) < 1/2$, we also have that $\hat{q}_i(L) < 2^{-L}$ by Equation (1); therefore, if $L < \min_i L_i^*$, $\hat{q}_i(L) < 2^{-L}$ for all $i \in [n]$. Subsequently, the expected false positive is also exponentially decreasing $\hat{F}(L) = \sum_{i=1}^n c_i \hat{q}_i(L) < \sum_{i=1}^n c_i 2^{-L} \leq n 2^{-L}$. \square

Remark. The region $[1, L_{\min}]$ covers a wide range of F_0 . Even in the worst case where $c_i = 1$, the region covers the expected number of false positives down as low as $n 2^{-L_{\min}} = n 2^{-\frac{B}{\max_i |W_i|} \ln 2}$, that is, $B \geq \frac{1}{\ln 2} \times \max_i |W_i| \times \log_2 \frac{n}{F_0}$ surely enables fast optimization via binary search on the strictly decreasing function. Nonetheless, alg. 1 measures a tighter expected false positive lower bound of the region $F(L_{\min})$ to decide whether to use fast optimization.

Lemma 3. For $L > \max_i L_i^* = L_{\max}$, expected false positive is strictly increasing $\hat{f}(L) > 0$.

Proof. If $L > L_i^*$, $z_i(L) > 1/2$. Together with Equation (3), it implies that $\hat{q}'_i(L) > 2^{-L-1} \ln \frac{z_i(L)}{1-z_i(L)} > 0$. \square

d) *False Positive Guarantee*: For fixed numbers of bins B and layers L , each false positive from i -th document on irrelevant query word w is a multiple of Bernoulli random variable, i.e. $x_{i,w} = p_w b_i$ where $b_i \sim \text{Bern}(q_i(L))$. Since $x_{i,w} \in [0, p_w]$ and $E[x_{i,w}] = p_w q_i(L)$, Hoeffding’s inequality guarantees that the observed number of false positives $X = \sum_{i=1}^n \sum_{w \in W \setminus W_i} x_{i,w}$ does not deviate more than the expectation $E[X] = F(L)$ by ε with probability at least $1 - \delta$.

$$\delta = \Pr[X \geq F(L) + \varepsilon] \leq \exp\left(-2\varepsilon^2/\sigma_X^2\right) \quad (5)$$

where $\sigma_X^2 = \sum_{i=1}^n \sum_{w \in W \setminus W_i} p_w^2$. Thus, the deviation is bounded with $\varepsilon \leq \sqrt{\frac{1}{2}\sigma_X^2 \ln \frac{1}{\delta}}$. In the worst case where very few query words are irrelevant to all documents and dominate the distribution ($p_w \rightarrow 1$) making $\sigma_X^2 \rightarrow n$, the deviation can possibly be as large as $\varepsilon \leq \sqrt{\frac{n}{2} \ln \frac{1}{\delta}} = O(\sqrt{n})$; however, a memoization technique such as query caching suffices to solve this case. It is worth noting that, in a typical case when there are many irrelevant query words with similar probability, the deviation would instead shrink as the number of words increases: $\varepsilon \leq \sqrt{\frac{n}{2|W|} \ln \frac{1}{\delta}} = O\left(\sqrt{\frac{n}{|W|}}\right)$.

As a point of reference, Table II summarizes corpus-dependent coefficients σ_X for each corpus in the experiment assuming query words distribute uniformly among relevant words found in corpus. To reiterate, this analysis only ensures the concentration of the observed number of false positives around $F(L)$. The number of false positives itself can be reduced by adjusting IoU Sketch’s structure (B, L).

B. Corpus Profiling

Although the optimization formulation factors in any categorical query word distribution w , AIRPHANT assumes a uniform distribution by default; in other words, a query equally likely contains words in the corpus or $p_w = 1/|W|$. While no further evidence support nor deny such choice, it is potentially simplistic. Other possible apparent choices with their profiling are: (a) $p_w = \text{occurrences}(w)$ by profiling word occurrences and total number of words, and (b) user-provided or statistical prior p_w with no profiling. One might also consider assigning non-zero $p_{w'}$ where $w' \notin W$. We defer seeking more suitable distributions to future studies and let this implementation be a case study. Subsequently, AIRPHANT Builder’s profiling then counts the number of distinct words in the corpus as well as the numbers of distinct words within each document.

C. Superpost Compaction

AIRPHANT Builder implements a simple superpost compaction to avoid creating too many tiny or a few huge files, and to allow single-cycle retrievals in AIRPHANT Searcher. Previously hinted in earlier sections, the compaction comprises of two components: a header block and superpost blocks.

Each of the superpost blocks stores serialized multiple superposts consecutively. AIRPHANT internally uses Protocol Buffers to serialize superposts to byte arrays. While indexing, AIRPHANT Builder keeps track of each superpost location and builds the dictionary of bin pointers. Given the superpost

block structure, each bin pointer need to represent block ID, offset, and byte length to retrieve the superpost’s bytes in a single round-trip. In addition, AIRPHANT compresses repeated strings within postings into integer keys. The compression reduces the number of bytes per superpost to be downloaded which speeds up query overall.

AIRPHANT Builder persists these bin pointers and string compression table along side with hash seeds and other metadata in the header block. The hash seeds are collected from the hash function in IoU Sketch; in other words, they concisely represents IoU Sketch mapping. It is this header block that is loaded on AIRPHANT Searcher initialization.

D. Top-K Query

Instead of retrieving all relevant documents in a query, AIRPHANT Searcher supports fetching at least K relevant documents. Top- K query enables pagination for providing a quick view or batch processing. Thanks to IoU Sketch’s false positive guarantee, that is, the approximated superpost contains F_0 irrelevant documents on average, AIRPHANT Searcher can sample a subset of the superpost to fetch from. Suppose the superpost contains R postings, if $K \geq R - F_0$, then AIRPHANT Searcher fetches all R documents. Otherwise, each posting corresponds to a relevant document with Bernoulli distribution $\text{Bern}(p = 1 - F_0/R)$. With probability at least $1 - \delta$, solving a quadratic inequality after applying Hoeffding’s inequality guarantees that sampled postings of size R_K (Equation (6)) comprise of at least K relevant documents.

$$R_K = \left\lceil \frac{2pK + \frac{1}{2} \ln \frac{1}{\delta} + \sqrt{(2pK + \frac{1}{2} \ln \frac{1}{\delta})^2 - 4p^2 K^2}}{2p^2} \right\rceil \quad (6)$$

E. Common Words

Common words are keywords that are contained in many documents in the corpus. Some information retrieval systems assign them as stop words and filter them out during all retrieval steps. In contrary, AIRPHANT supports searching for common words. The challenge is that, merging their large postings lists into IoU Sketch’s bins would deteriorate performance on other keyword query as well. As a workaround, AIRPHANT sets aside 1% of the bins to store the exact postings lists of most common words. For example, if $B = 10^5$, AIRPHANT would use 99,000 bins for IoU Sketch and 1,000 bins to carry 1,000 most common words’ postings lists. We use the same superpost compaction for these postings lists.

F. Applicable Queries

Although IoU Sketch only natively supports queries on a single term, we can adapt it to accelerate other classes of queries. For one, like an inverted index, IoU Sketch naturally generalizes to Boolean queries [32]. Let $Q(w)$ be the superpost from querying IoU Sketch with word w . IoU Sketch executes any Boolean query by distributing its query function to each term predicate $Q(\bigvee_i \bigwedge_j w_{ij}) = \bigcup_i \bigcap_j Q(w_{ij})$. In particular, intersection and union operators apply to superposts where the former reduces false positives and the latter adds. Furthermore,

regular expression (RegEx) can benefit from IoU Sketch as inverted index by considering indexing N -grams as shown in RegEx engines [33] [34]. These engines use an inverted index as a filter to avoid a full corpus scan, and later match the remaining documents with the RegEx to remove false positives. Hence, superpost’s false positives do not affect the final correctness.

G. Built-in Replication for Reliability

During its query execution, IoU Sketch retrieves superposts from all L layers simultaneously in parallel I/O requests. As a result, the slowest retrieval among L requests defines the total query latency, exposing IoU Sketch to the Long Tail Problem if there is any extreme variation during the I/Os such as dormant storage or network congestion [35]. Nonetheless, IoU Sketch’s multi-layer structure comes to the rescue as a built-in replication mechanism. The core idea is that IoU Sketch can simply discard the pending slow request and return the available-but-suboptimal superpost. The simplest mitigation is then to set a timeout before aborting the trailing request. Alternatively, IoU Sketch can enhance its reliability by overestimating the number layers, say L_+ , adding magnitudes of accuracy as a consequence. The more layers IoU Sketch overestimates, the stronger its reliability against long-tail requests becomes. During a query, IoU Sketch would then submit L_+ I/O requests but only wait for any L successful retrievals. We refer to [36] for more sophisticated techniques and analysis frameworks.

V. EXPERIMENTS

We have conducted empirical studies to evaluate AIRPHANT’s performance. We observe that:

1. AIRPHANT outperforms Lucene, Elasticsearch, SQLite, and HashTable with upto $8.97\times$, $113.39\times$, $3.15\times$, and $378.59\times$ faster response respectively (§V-B0a).
2. AIRPHANT competitively controls the effect of physical distance between compute and storage compared to baselines (§V-B0b).
3. Our latency analysis shows that baselines are slower due to either time spent being blocked waiting for network response or downloading large amount of data. AIRPHANT reduces both portions of time at the same time (§V-B0c).
4. With the separation of compute and storage, AIRPHANT is more cost-efficient than a Elasticsearch deployed with local persistence when the workload is skewed (high or rare peak throughput) and/or the size of indexed data is large (§V-C).
5. Our last experiments justify IoU Sketch analysis, showing that IoU Sketch provides a trade-off between memory usage and latency and that its structure optimization is crucial. (§V-D)

A. Environment Setup

Our experiments used Google Cloud Platform. It uses GCP Cloud Storage [8] as the cloud storage for index structure persistence. To provide file-system interface for all benchmarks, we connect all necessary storage buckets to a directory

TABLE II: Corpus Statistics. #documents: number of documents. #terms: number of distinct words. #words: total number of words across all documents. σ_X : corpus-dependent coefficient discussed in §IV-A.

| Corpus | #documents | #terms | #words | σ_X |
|---------------|-------------------|-------------------|-------------------|------------|
| diag(8, 8, 0) | 10^8 | 10^8 | 10^8 | 1.00 |
| unif(8, 8, 1) | 10^8 | 1.0×10^8 | 1.0×10^9 | 1.00 |
| zipf(8, 8, 1) | 10^8 | 5.0×10^7 | 9.5×10^8 | 1.41 |
| Cranfield | 1.4×10^3 | 5.3×10^3 | 1.2×10^5 | 0.51 |
| HDFS | 1.1×10^7 | 3.6×10^6 | 1.4×10^8 | 1.77 |
| Windows | 1.1×10^8 | 8.3×10^5 | 1.7×10^9 | 11.73 |
| Spark | 3.3×10^7 | 5.2×10^6 | 3.5×10^8 | 2.53 |

using Cloud Storage FUSE [37] (`gcsfuse`) adaptor with no limit on rate of operations. We allocate two VM instances `n2-highmem-32` (32 vCPUs, 256 GB memory, 1 TB SSD persistent disk) and `e2-small` (2 vCPUs, 2 GB memory, 10 GB default boot disk) for indexing and query benchmarking respectively. All experiments run from September to November 2021.

a) *Datasets*: There are 4 corpuses to benchmark these index systems. Cranfield (Cranfield 1400) [38] is a small corpus of 1398 documents, each contains abstracts from aerodynamics research papers. HDFS [39], Windows, and Spark are system logs in their corresponding systems collected by Loghub [40].

In addition, we use 3 types of synthetic datasets whose size is configurable. We denote the size of each synthetic dataset using a tuple $(\log_{10} n_d, \log_{10} n_w, \log_{10} n_l)$ for its numbers of documents n_d , words n_w , and words per documents n_l . `diag` is a dataset where each document i contains only one word w_i . As a result, `diag` always has $n_l = 1$. `unif` is a dataset where each word in a document is uniformly sampled from the n_w -word dictionary. `zipf` is similar to `unif` but uses a Zipfian distribution with the exponent equal to 1.07. In other word, each word in a document is equal to w_j with probability proportional to $1/j^{1.07}$. Note that `unif` and `zipf` can under-generate the actual set of distinct words form n_w due to Coupon collector’s problem [41]. Table II summarizes corpuses’ statistics that are used in §V-B0a.

b) *Baselines*: We compare AIRPHANT to Lucene 7.4.0 [19], Elasticsearch 7.15.1 [20], SQLite 3.34.0 [21], and naïve hash table. Lucene is an information retrieval library. Elasticsearch is a search and analytics engine. We benchmark their efficiency in matching exact keywords. We first parse keywords out similarly to other baselines and feed parsed documents to a text field using Elasticsearch’s `whitespace` analyzer and Lucene’s `WhitespaceAnalyzer` along with the document’s posting. To benchmark Elasticsearch, we mount a Searchable Snapshot [42] onto an Elasticsearch empty instance to speed up its initial latency.

SQLite is a light database we choose as a practical B-tree implementation. We first create a two-column table consisting of keyword column and postings column to mimic the inverted index dictionary. We then build SQLite’s B-tree index [43] on

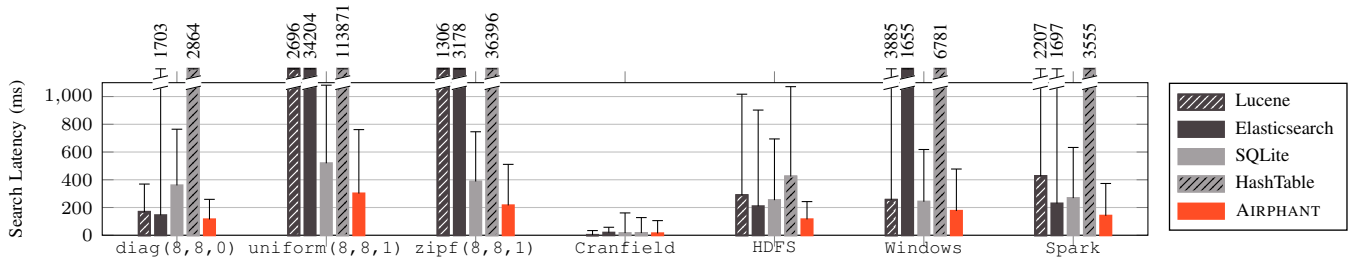


Fig. 6: End-to-end search latencies of indexes on different datasets. Solid bars show average latencies; the upper error bars show 99th percentiles. Latencies over 1.1 seconds are truncated and labeled. 99 percentiles whose means are over the limit are omitted.

the keyword column as its term index and store its database file on the cloud-mounted directory. In each query, after retrieving the postings, SQLite reuses the same document retrieval routine from AIRPHANT.

Lastly, HashTable refers to an inverted index that stores postings lists according to their corresponding terms’ hashes. It is equivalent to IoU Sketch with the only exception that it has a single layer $L = 1$. Other relevant configurations such as the total number of bins and common word bins are identical to IoU Sketch. All postings inserted in all baselines are compressed in the same way as in AIRPHANT (§IV-C).

c) Parameters: If otherwise specified, we set the number of bins $B = 10^5$, accuracy constraint $F_0 = 1$, and probability of top- K query failure $\delta = 10^{-6}$ for $K = 10$. Remind that we allocate 1% of the bins to store postings lists of most common words. We similarly set top- K query to other baselines accordingly. The top- K query failure never occurs during the experiment due to the conservative setting which selects about 23 samples to answer top-10 query. The accuracy choice leads to optimal number of layers L^* in the at most 3 layers depending on the corpus. The number of bins results in AIRPHANT Search’s runtime size about 2 MB. We use 32 threads to concurrently read any data from the cloud storage.

B. End-to-end Search Performance

a) Within Region: To demonstrate AIRPHANT’s performance, we measure end-to-end search latency for each query. Figure 6 shows mean and 99th-percentile latencies. AIRPHANT query executions are $1.45\times$ to $8.97\times$ faster than Lucene’s on average (except Cranfield dataset where Lucene is $8.00\times$ faster), $1.09\times$ to $113.39\times$ faster than Elasticsearch’s, $1.12\times$ to $3.15\times$ faster than SQLite’s, and $1.15\times$ to $378.59\times$ faster than HashTable’s. HashTable is slow because it spends the majority of its latency to filter out false-positive documents, which highlights the strength of IoU Sketch’s multi-layer structure.

From these benchmarks, we see that AIRPHANT operates at less than 300 ms on average. According to [44], [45], web search users start to notice the latency when it is on the order of seconds, and so, they are tolerable with AIRPHANT latency. To put its latency into a perspective, AIRPHANT would only add a factor to the 250 ms “speed-of-light web search latency”.

b) Cross Region: Separation of compute and storage allows AIRPHANT to host each component in different physical locations, even across continents. To construct such a

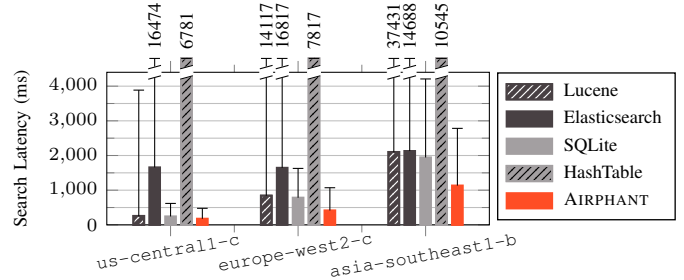


Fig. 7: End-to-end search latencies across regions of indexes. The Windows dataset was used. Solid bars show average latencies; the upper error bars show 99th percentiles of measured latencies.

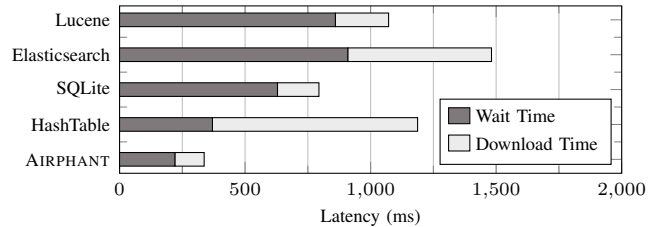


Fig. 8: Search latency breakdown in terms of network communication on the Spark dataset. The total search latency is equal to the summation of wait time and download time.

scenario, we allocate a cloud storage in the default US (multi-region US), while hosting VMs at us-centrall-c (Iowa), europe-west2-c (London), and asia-southeast1-b (Singapore). Because we observe similar performance patterns across all datasets, Figure 7 only presents Windows as a representative. It comes as no surprise that each method takes longer as its VM moves further from the data. Among those baselines with competitive latencies, Lucene is $3.3\times$ and $8.2\times$ slower and SQLite is $3.2\times$ and $8.0\times$ slower in London and Singapore. In contrast, AIRPHANT achieves a milder slowdown: $2.4\times$ and $6.5\times$ ($3.3\times$ and $6.8\times$ across all datasets, not shown). Elasticsearch and HashTable, on the other hand, are consistently slower than others, across different regions: Elasticsearch spends much time in mounting its searchable snapshots; HashTable reads too many false positives.

c) Latency Breakdown: To dig deeper, we study data movement patterns from the perspective of network communication via TCP packets captured by tcpdump⁶. We sample

⁶<https://www.tcpdump.org>

32 queries from each method, capture packets on appropriate ports. We then compute two metrics per query: waiting time and download time.⁷ We calculate bandwidth usage based on moving averages of the size of packets with window size of 10 ms. Figure 8 depicts the result of this procedure. Note that the latency is slower than those in Figure 6 partly due to `tcpdump` and a smaller number of query samples. There are two opposite patterns among baselines. First, as we have mentioned, HashTable’s latency dominantly consists of time to download false-positive documents. Secondly and conversely, Lucene and SQLite tend to wait for their dependent reads, i.e. B-tree or skip list traversal. AIRPHANT minimizes such dependency thanks to the independence among IoU Sketch’s layers, reducing wait time as a result. AIRPHANT also improves download time because of its parallel I/O reads which utilizes more network bandwidth. AIRPHANT spends 220ms waiting and 117ms downloading on average where its breakdown distribution concentrates around.

C. Cost Comparison

This experiment compares costs between the two architecture paradigms: coupled (compute and storage adjacency) and decoupled (compute and storage separation). To this end, we consider the *peak-trough* workload that elucidates the trade-off between the two paradigms. The peak-trough workload is motivated by the periodically varying utilization commonly found in web services. As the name suggests, it consists of two parts: peak and trough. Peak refers to the time where the workload is higher, whereas trough’s workload is lower. Because our following cost formulae are linear on the amount of time, we can identify a peak-trough instance with (A, a, τ) where peak and trough cover τ and $1 - \tau$ fraction of time with workload A and a ops/s respectively.

Furthermore, we also consider the total number of corpora. For simplicity, we consider a collection of corpora whose document-word pairs are distributed similarly to `Windows`. We denote S as the total size of original data in bytes. Estimated from their storage usage in `Windows`, AIRPHANT uses $1.008 \times S$ bytes, while Elasticsearch has a better compression rate and only uses $0.3316 \times S$ bytes of storage.

Since AIRPHANT can scale up/down easily as per workloads, AIRPHANT costs proportionally to the workload over time: $O(a_p t + a_t(1 - t))$. From previous performance results, AIRPHANT operates at 175 ms/op or 5.71 ops/s. Deploying AIRPHANT on `e2-small` VM costs \$13.23/month, and storing its index on GCP Cloud Storage costs \$0.02/GB/month.

In contrast, Elasticsearch cannot automatically scale down without rebalancing its index over remaining servers; as a result, it requires the resource to handle the peak workload at all times, amounting to $O(a_p)$ cost. Nonetheless, we optimistically assume that Elasticsearch’s sharding and load balancing are perfect such that its throughput scales linearly with the number of servers without shard replication. We deploy Elasticsearch

⁷The former includes the time when the bandwidth usage is less than 10 kB/s while the latter includes the rest where the traffic is high.

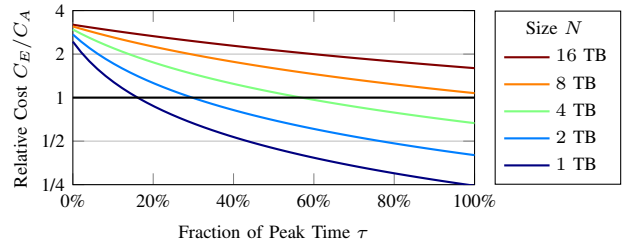


Fig. 9: Relative cost between local Elasticsearch and cloud-stored AIRPHANT in terms of fraction of peak time τ and size of indexed data N (increasing from bottom to top lines). Peak and trough workloads are fixed to $A = 154.08$ op/s (throughput of a single Elasticsearch server) and $a = A/20 = 7.704$ op/s.

on `e2-medium` VM (\$26.46/month) and store its index on local disk (\$0.2/GB/month). This achieves 6.49 ms/op and is the most cost-efficient among the options we explored.

Figure 9 shows a slice of the relative cost C_E/C_A at fixed A and a . Overall, AIRPHANT costs less if the total corpus size N is larger and/or the fraction of peak time τ is smaller. In fact, we would asymptotically save $\lim_{N \rightarrow \infty} C_E/C_A \approx 3.29$ times of the cost of coupled Elasticsearch. Also, focusing on the VM cost, AIRPHANT’s cost would be $A/(13.48a)$ times over Elasticsearch’s. A relatively higher peak workload $A > 13.48a$ implies that a relatively lower cost to deploy AIRPHANT, and vice versa. These trends align with the intuition: the decouple paradigm is more cost-efficient than coupled one when 1) the data is large, 2) the workload is concentrated over peak times, and/or 3) the peak’s workload is high compared to trough’s.

D. IoU Sketch Structure

We use `HDFS` to explore $B \in \{50k, 100k, 200k, 400k\}$ around the configuration used in §V-B0a and a wide range of $L \in \{1, 2, 4, 6, 8, \dots, 16\}$. Recall that $L = 1$ corresponds to the naïve hash table index structure and note that our optimizer selects $L^* = 2$. Figure 10a confirms our analysis which predicts a rapid error reduction over L given a sufficient B ; the observed average numbers of false positives are enormous at $L = 1$, become less than 1 at $L = 2$, and are exactly zero after $L = 4$. Such high numbers of false positives in $L = 1$ result in a higher search latency (Figure 10b) due to heavy filtering demands. The rest of the search latency trend correlates closely with the term lookup latency (Figure 10c); when L increases, so does the lookup latency. Even though AIRPHANT fetches superposts in layers separately, a bandwidth contention drives up the lookup latency and search latency as a result.

VI. RELATED WORK

A. Data Systems in the Cloud

Cloud services provide a convenient interface to share computing resources. As one of its most important impact, the cost of scaling up or down is now low enough that elasticity, or ability to scale to meet the demand, is a desirable feature of a system. Some work achieves elasticity through separation of compute and storage. Particularly, applications that are functional or can be partitioned into smaller functional

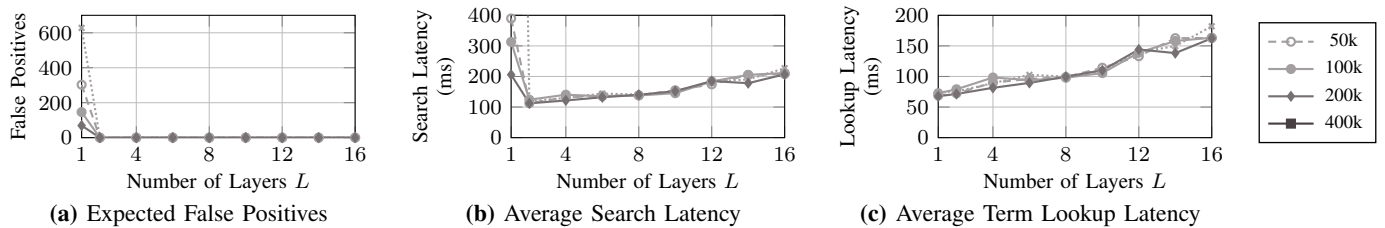


Fig. 10: Effects of numbers of bins B and layers L on expected number of false positives (in logarithmic scale), average search latency, and average term lookup latency, from left to right. Each line corresponds to a number of bins $B \in \{50k, 100k, 200k, 400k\}$, while x-axis corresponds to the number of layers L . Average search latency (not shown) for $(B = 50k, L = 1)$ is 3,556 ms. The underlying corpus is HDFS.

modules enjoy elasticity by FaaS [46]. Apart from web serving and file processing, `gg` framework [47] empowers FaaS execution for commonly local applications, for example, video encoding, object recognition, unit testing. Towards FaaS-based query engine, Starling [48] partitions a query into fine-grained tasks on operation level such as table scanning, joining, and shuffling. AIRPHANT partitions a functional searching into AIRPHANT Searcher, and persists index data structure stored on cloud storage. In this way, AIRPHANT can also benefit from FaaS elasticity.

B. Index Data Structures

a) Sketches: [49] lays out numerous sketch techniques. Most notably similar sketches to IoU Sketch sketches are count-min sketch [50] and Bloom filter [51]. IoU Sketch and count-min sketch both maintain a multi-layer hash table and answer queries using aggregations. Bloom filter’s accuracy formulation is similar to IoU Sketch’s counterpart; however, IoU Sketch focuses on maximizing its retrieval performance using its accuracy term as one of the constraints while Bloom filter directly maximizes its accuracy. Moreover, Bloom filter has a closed-form optimal configuration, but IoU Sketch’s can contain multiple local optima.

b) Hash Tables: Open addressing probes for available entries to insert colliding values accordingly to a mechanism, for example, Hopscotch [52], SmartCuckoo [53], and Min-Counter [54]. Open addressing performs well when load factor is low [55], which is infeasible with a memory constraint.

Unlike B-trees, hash table is popular in distributed peer-to-peer systems, especially for point-query indexing. Each solution differs from others based on its query routing [56], such as tree-like (Pastry [57], Tapestry [58], Kademlia [59]) or skip-list-like (Chord [60], Koorde [61]). A keyword searching application can rely on these systems to store and retrieve postings lists; however, it would require long-running servers equipped with storage, as opposed to our serverless system.

c) Hierarchical Indexes: B-tree [12] is widely used due to its efficiency, self-balancing, and cheap reorganization [62]. Many B-tree variants and techniques optimize B-tree across memory levels and storage mediums, e.g. CPU cache [63], SRAM cache [14], disk [13], SSD [64], NVMe [65], and distributed systems [66]–[68].

Skip list is another index structure based on linked list with skip connections. Like B-trees, many skip lists are optimized to various settings, such as multi-core [69], cache-sensitive for range queries [70], non-uniform access [71], and distributed nodes [72]. Skip list can be combined with other data structures as well: hash table [60], [61], search tree [73], multi-dimensional octree [74], and compressed perfect skip list for inverted index [75].

However, these hierarchical index structure can be inefficient in our cloud setting when corpus size is large. Although [76] suggests increasing the effective fan-out, a server with limited memory still requires multiple sequential round-trips. A workaround is to increase the server’s memory capacity, thereby incurring extra costs. AIRPHANT achieves single round-trip per query even on a memory-constrained node.

C. Approximation Techniques for Data Systems

Besides sketching (§VI-B), approximation and learning-based techniques have been proposed to speed up large-scale data analytics [77]–[83], selectivity estimation [84]–[87], etc. and to automate database tuning [88]–[90], etc. In contrast, AIRPHANT develops a novel statistical inverted index for document stores.

VII. CONCLUSION

This work presents AIRPHANT, a search engine developed to achieve low end-to-end query latencies under the separation of compute and storage. While AIRPHANT keeps almost the entire data on cloud storage (both inverted index and original documents), it delivers search results within 300 milliseconds. This is a significant improvement compared to placing existing search engines directly on top of cloud storage. At its core, AIRPHANT relies on our new statistical inverted indexing technique called IoU Sketch. Unlike many other existing indexes, IoU Sketch does not require sequential back-to-back communications with storage devices. With IoU Sketch, we can make a single batch of concurrent communications, which significantly lowers the end-to-end wall clock time in obtaining relevant documents (i.e., the documents containing search keywords). We plan to open-source this technology (and AIRPHANT itself) after enhancing its index building component (for higher scalability) and also making it more extensible for diverse public cloud environments.

VIII. ACKNOWLEDGEMENT

This work is supported in part by Microsoft Azure and Google Cloud Platform.

REFERENCES

- [1] B. Dageville, T. Cruanes, M. Zukowski, V. Antonov, A. Avanes, J. Bock, J. Claybaugh, D. Engovatov, M. Hentschel, J. Huang *et al.*, “The snowflake elastic data warehouse,” in *Proceedings of the 2016 International Conference on Management of Data*, 2016, pp. 215–226.
- [2] G. Cloud, “BigQuery: Cloud data warehouse,” <https://cloud.google.com/bigquery>, [Online; accessed April-14-2021].
- [3] A. W. Services, “Amazon Redshift: Cloud data warehouse,” <https://aws.amazon.com/redshift/?whats-new-cards.sort-by=item.additionalFields.postDateTime&whats-new-cards.sort-order=desc>, [Online; accessed April-14-2021].
- [4] PrestoDB, “Distributed sql query engine for big data,” <https://prestodb.io/>, [Online; accessed April-14-2021].
- [5] Trino, “Distributed sql query engine for big data,” <https://trino.io/>, [Online; accessed April-14-2021].
- [6] A. W. Services, “Cloud object storage,” <https://aws.amazon.com/s3/>, [Online; accessed April-14-2021].
- [7] M. Azure, “Azure blob storage,” <https://azure.microsoft.com/en-us/services/storage/blobs/>, [Online; accessed April-14-2021].
- [8] G. Cloud, “Cloud storage,” <https://cloud.google.com/storage>, [Online; accessed April-14-2021].
- [9] C. B. Paul R. La Monica, “Snowflake shares more than double. it’s the biggest software ipo ever,” <https://www.cnn.com/2020/09/16/investing/snowflake-ipo/index.html>, [Online; accessed May-01-2021].
- [10] A. AWS, “Amazon redshift introduces ra3 nodes,” <https://aws.amazon.com/about-aws/whats-new/2019/12/amazon-redshift-announces-ra3-nodes-managed-storage/>, [Online; accessed April-14-2021].
- [11] W. Pugh, “Skip lists: a probabilistic alternative to balanced trees,” *Communications of the ACM*, vol. 33, no. 6, pp. 668–676, 1990.
- [12] R. Bayer and E. M. McCreight, “Organization and maintenance of large ordered indexes,” *Acta Informatica*, vol. 1, pp. 173–189, 1972.
- [13] S. Chen, P. B. Gibbons, T. C. Mowry, and G. Valentin, “Fractal prefetching b+-trees: Optimizing both cache and disk performance,” 2002.
- [14] S. Chen, P. B. Gibbons, and T. C. Mowry, “Improving index performance through prefetching,” *SIGMOD Record (ACM Special Interest Group on Management of Data)*, vol. 30, 2001.
- [15] T. Kraska, A. Beutel, E. H. Chi, J. Dean, and N. Polyzotis, “The case for learned index structures,” 2018.
- [16] J. Ding, U. F. Minhas, J. Yu, C. Wang, J. Do, Y. Li, H. Zhang, B. Chandramouli, J. Gehrke, D. Kossmann, D. Lomet, and T. Kraska, “Alex: An updatable adaptive learned index,” 2020.
- [17] A. Bialecki, R. Muir, G. Ingersoll, and L. Imagination, “Apache lucene 4,” in *SIGIR 2012 workshop on open source information retrieval*, 2012, p. 17.
- [18] ElasticSearch, “S3 repository plugin,” <https://www.elastic.co/guide/en/elasticsearch/plugins/current/repository-s3.html>, [Online; accessed April-14-2021].
- [19] A. Lucene, “Apache lucene,” <https://lucene.apache.org>, [Online; accessed April-24-2021].
- [20] ElasticSearch, “Free and open search: The creators of elasticsearch, elk & kibana,” <https://www.elastic.co/>, [Online; accessed April-14-2021].
- [21] SQLite, “SQLite,” <https://www.sqlite.org>, [Online; accessed April-24-2021].
- [22] H. Schütze, C. D. Manning, and P. Raghavan, *Introduction to information retrieval*. Cambridge University Press Cambridge, 2008, vol. 39.
- [23] A. Lucene, “Package org.apache.lucene.codecs,” https://lucene.apache.org/core/8_1_0/core/org/apache/lucene/codecs/package-summary.html, [Online; accessed May-01-2021].
- [24] P. Kirschenhofer, C. Martínez, and H. Prodinger, “Analysis of an optimized search algorithm for skip lists,” *Theoretical Computer Science*, vol. 144, no. 1-2, pp. 199–220, 1995.
- [25] D. Smiley, E. Pugh, K. Parisa, and M. Mitchell, *Apache Solr enterprise search server*. Packt Publishing Ltd, 2015.
- [26] G. Cloud, “Http headers and query string parameters for xml api,” <https://cloud.google.com/storage/docs/xml-api/reference-headers#range>, [Online; accessed April-20-2021].
- [27] A. W. Service, “Use byte-range fetches,” <https://docs.aws.amazon.com/whitepapers/latest/s3-optimizing-performance-best-practices/use-byte-range-fetches.html>, [Online; accessed April-20-2021].
- [28] M. Azure, “Specifying the range header for blob service operations,” <https://docs.microsoft.com/en-us/rest/api/storageservices/specifying-the-range-header-for-blob-service-operations>, [Online; accessed April-20-2021].
- [29] G. Cloud, “Cloud functions,” <https://cloud.google.com/functions>, [Online; accessed April-20-2021].
- [30] A. W. Service, “Aws lambda,” <https://aws.amazon.com/lambda/>, [Online; accessed April-20-2021].
- [31] M. Azure, “Azure functions,” <https://azure.microsoft.com/en-us/services/functions/>, [Online; accessed April-24-2021].
- [32] C. D. Manning, P. Raghavan, and H. Schütze, *Introduction to Information Retrieval*. USA: Cambridge University Press, 2008.
- [33] T. Qiu, X. Yang, B. Wang, and W. Wang, “Efficient regular expression matching based on positional inverted index,” *IEEE Transactions on Knowledge and Data Engineering*, pp. 1–1, 2020.
- [34] J. Cho and S. Rajagopalan, “A fast regular expression indexing engine,” in *Proceedings 18th International Conference on Data Engineering*, 2002, pp. 419–430.
- [35] S. S. Gill, X. Ouyang, and P. Garraghan, “Tails in the cloud: a survey and taxonomy of straggler management within large-scale cloud data centres,” *The Journal of Supercomputing*, pp. 1–40, 2020.
- [36] D. Wang, G. Joshi, and G. W. Wornell, “Efficient straggler replication in large-scale parallel computing,” *ACM Transactions on Modeling and Performance Evaluation of Computing Systems (TOMPECS)*, vol. 4, pp. 1 – 23, 2019.
- [37] G. Cloud, “Cloud storage fuse,” <https://cloud.google.com/storage/docs/gcs-fuse>, [Online; accessed April-14-2021].
- [38] C. Cleverdon, “The cranfield tests on index language devices,” 1967.
- [39] W. Xu, L. Huang, A. Fox, D. Patterson, and M. I. Jordan, “Detecting large-scale system problems by mining console logs,” 2009.
- [40] S. He, J. Zhu, P. He, and M. R. Lyu, “Loghub: A large collection of system log datasets towards automated log analytics,” 2020.
- [41] P. Flajolet, D. Gardy, and L. Thimonier, “Birthday paradox, coupon collectors, caching algorithms and self-organizing search,” *Discrete Applied Mathematics*, vol. 39, no. 3, pp. 207–229, 1992. [Online]. Available: <https://www.sciencedirect.com/science/article/pii/0166218X9290177C>
- [42] ElasticSearch, “Elasticsearch searchable snapshots,” <https://www.elastic.co/elasticsearch/elasticsearch-searchable-snapshots/>, [Online; accessed October-30-2021].
- [43] SQLite, “Database file format,” <https://www.sqlite.org/fileformat.html>, [Online; accessed April-20-2021].
- [44] J. D. Brutlag, H. B. Hutchinson, and M. Stone, “User preference and search engine latency,” 2008.
- [45] I. Arapakis, S. Park, and M. Pielot, “Impact of response latency on user behaviour in mobile web search,” *Proceedings of the 2021 Conference on Human Information Interaction and Retrieval*, 2021.
- [46] J. Schleier-Smith, “Serverless foundations for elastic database systems,” 2019.
- [47] S. Fouladi, F. Romero, D. Iter, Q. Li, S. Chatterjee, C. Kozyrakis, M. Zaharia, and K. Winstein, “From laptop to lambda: Outsourcing everyday jobs to thousands of transient functional containers,” 2019.
- [48] M. Perron, R. C. Fernandez, D. Dewitt, and S. Madden, “Starling: A scalable query engine on cloud functions,” 2020.
- [49] G. Cormode, “Sketch techniques for approximate query processing,” in *Synopses for Approximate Query Processing: Samples, Histograms, Wavelets and Sketches, Foundations and Trends in Databases. NOW publishers*, 2011.
- [50] G. Cormode and S. Muthukrishnan, “An improved data stream summary: The count-min sketch and its applications,” *Journal of Algorithms*, vol. 55, 2005.
- [51] B. H. Bloom, “Space/time trade-offs in hash coding with allowable errors,” *Communications of the ACM*, vol. 13, 1970.
- [52] M. Herlihy, N. Shavit, and M. Tzafrir, “Hopscotch hashing,” vol. 5218 LNCS, 2008.
- [53] Y. Sun, Y. Hua, S. Jiang, Q. Li, S. Cao, and P. Zuo, “Smartcuckoo: A fast and cost-efficient hashing index scheme for cloud storage systems,” 2019.
- [54] Y. Sun, Y. Hua, D. Feng, L. Yang, P. Zuo, and S. Cao, “Mincounter: An efficient cuckoo hashing scheme for cloud storage systems,” vol. 2015-August, 2015.

- [55] S. Richter, V. Alvarez, and J. Dittrich, "A seven-dimensional analysis of hashing methods and its implications on query processing," 2016.
- [56] H. Balakrishnan, M. F. Kaashoek, D. Karger, R. Morris, and I. Stoica, "Looking up data in p2p systems," 2003.
- [57] A. Rowstrom and P. Druschel, "Storage management and caching in past, a large-scale, persistent peer-to-peer storage utility," *Operating Systems Review (ACM)*, vol. 35, 2001.
- [58] K. Hildrum, J. D. Kubiawicz, S. Rao, and B. Y. Zhao, "Distributed object location in a dynamic network," 2002.
- [59] P. Maymounkov and D. Mazières, "Kademlia: A peer-to-peer information system based on the xor metric," *Lecture Notes in Computer Science (including subseries Lecture Notes in Artificial Intelligence and Lecture Notes in Bioinformatics)*, vol. 2429, 2002.
- [60] I. Stoica, R. Morris, D. Karger, M. F. Kaashoek, and H. Balakrishnan, "Chord: A scalable peer-to-peer lookup service for internet applications," vol. 31, 2001.
- [61] M. F. Kaashoek and D. R. Karger, "Koorde: A simple degree-optimal distributed hash table," *Lecture Notes in Computer Science (including subseries Lecture Notes in Artificial Intelligence and Lecture Notes in Bioinformatics)*, vol. 2735, 2003.
- [62] D. Comer, "Ubiquitous b-tree," *Comput Surv*, vol. 11, 1979.
- [63] G. Graefe and P. Åke Larson, "B-tree indexes and cpu caches," *Proceedings - International Conference on Data Engineering*, 2001.
- [64] R. Jin, S. J. Kwon, and T. S. Chung, "Flashb-tree: A novel b-tree index scheme for solid state drives," 2011.
- [65] L. Wang, Z. Zhang, B. He, and Z. Zhang, "Pa-tree: Polled-mode asynchronous b+ tree for nvme," vol. 2020-April, 2020.
- [66] S. Wu, D. Jiang, B. C. Ooi, and K. Wu, "Efficient btree based indexing for cloud data processing," *Proceedings of the VLDB Endowment*, vol. 3, 2010.
- [67] W. Zhou, J. Lu, Z. Luan, S. Wang, G. Xue, and S. Yao, "Snb-index: A skipnet and b+ tree based auxiliary cloud index," *Cluster Computing*, vol. 17, 2014.
- [68] H. Bin and P. Yuxing, "An efficient distributed b-tree index method in cloud computing," *Open Cybernetics and Systemics Journal*, vol. 8, 2014.
- [69] I. Dick, A. Fekete, and V. Gramoli, "A skip list for multicore," *Concurrency Computation*, vol. 29, 2017.
- [70] S. Sprenger, S. Zeuch, and U. Leser, "Cache-sensitive skip list: Efficient range queries on modern cpus," vol. 10195 LNCS, 2017.
- [71] H. Daly, A. Hassan, M. F. Spear, and R. Palmieri, "Numask: High performance scalable skip list for numa," vol. 121, 2018.
- [72] J. He, S. wen Yao, L. Cai, and W. Zhou, "Slc-index: A scalable skip list-based index for cloud data processing," *Journal of Central South University*, vol. 25, 2018.
- [73] J. Zhang, S. Wu, Z. Tan, G. Chen, Z. Cheng, W. Cao, Y. Gao, and X. Feng, "S3: A scalable in-memory skip-list index for key-value store," vol. 12, 2018.
- [74] "Dynamic multidimensional index for large-scale cloud data," *Journal of Cloud Computing*, vol. 5, 2016.
- [75] P. Boldi and S. Vigna, "Compressed perfect embedded skip lists for quick inverted-index lookups," vol. 3772 LNCS, 2005.
- [76] G. Graefe, "Modern b-tree techniques," *Foundations and Trends in Databases*, vol. 3, 2010.
- [77] Y. Park, A. S. Tajik, M. Cafarella, and B. Mozafari, "Database learning: Toward a database that becomes smarter every time," in *Proceedings of the 2017 ACM International Conference on Management of Data*, 2017, pp. 587–602.
- [78] T. Kraska, M. Alizadeh, A. Beutel, H. Chi, A. Kristo, G. Leclerc, S. Madden, H. Mao, and V. Nathan, "Sagedb: A learned database system," in *CIDR*, 2019.
- [79] Y. Park, B. Mozafari, J. Sorenson, and J. Wang, "Verdictdb: Universalizing approximate query processing," in *Proceedings of the 2018 International Conference on Management of Data*, 2018, pp. 1461–1476.
- [80] W. He, Y. Park, I. Hanafi, J. Yatvitskiy, and B. Mozafari, "Demonstration of verdictdb, the platform-independent aqp system," in *Proceedings of the 2018 International Conference on Management of Data*, 2018, pp. 1665–1668.
- [81] J. Bater, Y. Park, X. He, X. Wang, and J. Rogers, "Saqe: practical privacy-preserving approximate query processing for data federations," *Proceedings of the VLDB Endowment*, vol. 13, no. 12, pp. 2691–2705, 2020.
- [82] Y. Park, J. Qing, X. Shen, and B. Mozafari, "Blinkml: Efficient maximum likelihood estimation with probabilistic guarantees," in *Proceedings of the 2019 International Conference on Management of Data*, 2019, pp. 1135–1152.
- [83] Y. Park, M. Cafarella, and B. Mozafari, "Visualization-aware sampling for very large databases," in *2016 IEEE 32nd International Conference on Data Engineering (ICDE)*. IEEE, 2016, pp. 755–766.
- [84] Z. Yang, E. Liang, A. Kamsetty, C. Wu, Y. Duan, X. Chen, P. Abbeel, J. M. Hellerstein, S. Krishnan, and I. Stoica, "Deep unsupervised cardinality estimation," *Proceedings of the VLDB Endowment*, vol. 13, no. 3.
- [85] R. Marcus, P. Negi, H. Mao, C. Zhang, M. Alizadeh, T. Kraska, O. Papaemmanouil, and N. Tatbul23, "Neo: A learned query optimizer," *Proceedings of the VLDB Endowment*, vol. 12, no. 11.
- [86] Y. Park, S. Zhong, and B. Mozafari, "Quicksel: Quick selectivity learning with mixture models," in *Proceedings of the 2020 ACM SIGMOD International Conference on Management of Data*, 2020, pp. 1017–1033.
- [87] A. Kipf, T. Kipf, B. Radke, V. Leis, P. Boncz, and A. Kemper, "Learned cardinalities: Estimating correlated joins with deep learning," *arXiv preprint arXiv:1809.00677*, 2018.
- [88] J. Zhang, Y. Liu, K. Zhou, G. Li, Z. Xiao, B. Cheng, J. Xing, Y. Wang, T. Cheng, L. Liu *et al.*, "An end-to-end automatic cloud database tuning system using deep reinforcement learning," in *Proceedings of the 2019 International Conference on Management of Data*, 2019, pp. 415–432.
- [89] D. Van Aken, A. Pavlo, G. J. Gordon, and B. Zhang, "Automatic database management system tuning through large-scale machine learning," in *Proceedings of the 2017 ACM International Conference on Management of Data*, 2017, pp. 1009–1024.
- [90] Y. Zhu, J. Liu, M. Guo, Y. Bao, W. Ma, Z. Liu, K. Song, and Y. Yang, "Bestconfig: tapping the performance potential of systems via automatic configuration tuning," in *Proceedings of the 2017 Symposium on Cloud Computing*, 2017, pp. 338–350.

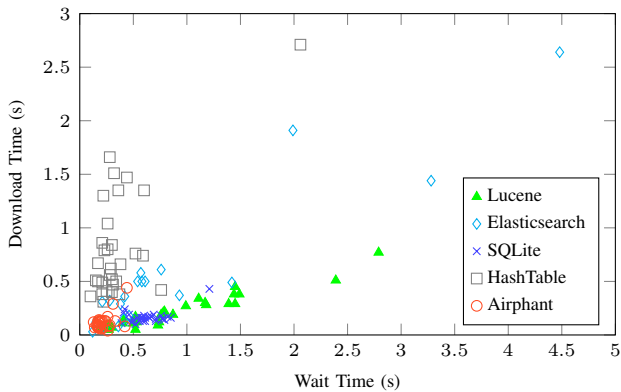


Fig. 11: Individual search latency breakdown in terms of network communication on the `Spark` dataset. Each scatter mark represents how long each individual search spends waiting and downloading. The total search latency is equal to the summation of wait time and download time. Faster searches reside in the lower left corner.

APPENDIX A ADDITIONAL VISUALIZATIONS

Here we include additional visualizations that we trim in the main sections due to space limitation.

A. Individual Latency Breakdown

§V-B0c summarizes search latency breakdown averages. Figure 11 instead visualizes latency breakdowns for individual search queries across systems. Most visibly perhaps is the fact that search latencies vary across queries due to many factors such as the result size, network variability, or buffer pool state. Nevertheless, the underlying search engine significantly dictates the breakdown. Overall, AIRPHANT outperforms other systems by minimizing both wait time and download time simultaneously.

On a closer look, this scatter plot reveals two extreme access patterns. First, wait-heavy systems (e.g. Lucene) spend most of the search waiting for network responses. The most probable culprit is their dependent sequential reads, that is, reads whose locations depend on decisions in preceding reads. For example, skip list traversal requires the current node to find the next node to skip to; therefore, to know which block to read next, the skip list needs to complete reading the current node first. Second, download-heavy systems (e.g. HashTable) spends most of the search downloading their data. These systems minimize their number of roundtrips but consume more data. In particular, HashTable (i.e. IoU Sketch where $L = 1$) contains a large number of false positives due to its limited filtering power. As a result, it unnecessarily reads a lot more false-positive documents but avoids roundtrips thanks to prefetching.

B. Full Cross-Region Results

§V-B0b shows search latency trends as we move further away from the cloud storage; however, it only selects those

measurements based on `Windows` dataset as the representative. Figure 12 and Figure 13 fully display the measurements across all 7 datasets.

APPENDIX B ADDITIONAL RESULTS

In contrary to the main results, we collect the following results from March to April 2021. Some measurements might disagree with those in earlier sections.

A. Term Index Lookup Performance

How does AIRPHANT achieve faster latencies? Recall that AIRPHANT and SQLite share the same document retrieval routine, so the difference in their latencies comes from the differences in both term index lookup operations and amounts of retrieved documents. Although AIRPHANT would need to retrieve more documents to take into account the false positives, its lookup speed gain justifies additional costs. Figure 14 reiterates the importance of AIRPHANT’s single-round-trip lookup operation. It evidently outperforms SQLite’s cached B-tree traversal both on average and at tail latency. In the best case, AIRPHANT is upto $2.79\times$ faster on average and $2.81\times$ faster at 99th percentile of term index lookup than SQLite.

B. Scalability with Corpus Size

We conduct a scalability experiment where we vary the size of synthetic datasets. In particular, we generate 17 datasets from `diag`, `unif`, and `zipf` by varying both numbers of documents n_d and distinct words n_w ranging from 10^3 to 10^8 . Figure 15 summarizes the measurement results of search latency and the index storage usage on `zipf` datasets. Results from `diag` and `unif` datasets possess the same pattern. It confirms that when the corpus is small, the baselines are faster, suggesting a room for AIRPHANT’s improvement in more aggressive caching policy. As the size of corpus increases, AIRPHANT relatively outperforms more and more across all synthetic datasets. The performance at the high end is summarized in previous section §V-B0a. In terms of storage size, AIRPHANT generally allocates more space comparing to both SQLite and Lucene but all follow the same trend in a logarithmic scale. In the worst setting, AIRPHANT uses $2.85\times$ more storage than Lucene.

C. Tiny IoU Sketch Structure

Apart from §V-D, we also use `Cranfield` to explore a restrictive range of $B \in \{1000, 1500, \dots, 3000\}$ and a excessively wide one for $L \in \{1, 2, 4, 6, 8, \dots, 16\}$. Recall that $L = 1$ corresponds to the naïve hash table index structure. Figure 16 shows four aspects of measurement. The false positive averages (Figure 16a) confirm our formulation: for a fixed B , there exists some L^* that minimizes the error. As B increases, we see the false positive averages decrease across all L . Such high numbers of false positives result in a higher search latency (Figure 16b) observed near the two ends of dotted line. Although the search latencies across different B

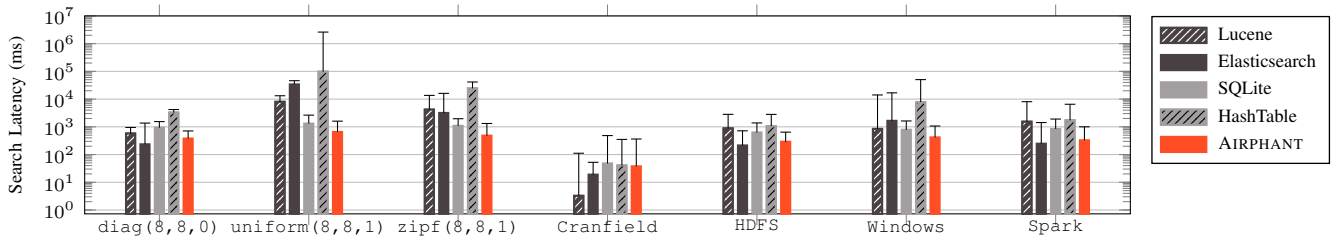


Fig. 12: End-to-end search latencies of indexes on different datasets from *Europe (London)*. Solid bars show average latencies while the upper error bars show 99th percentiles of measured latencies. Notice the logarithmic scale on the y-axis.

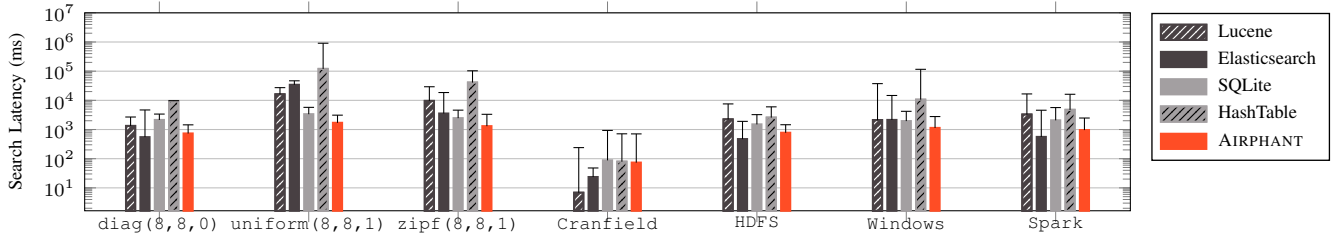


Fig. 13: End-to-end search latencies of indexes on different datasets from *Asia (Singapore)*. Solid bars show average latencies while the upper error bars show 99th percentiles of measured latencies. Notice the logarithmic scale on the y-axis.

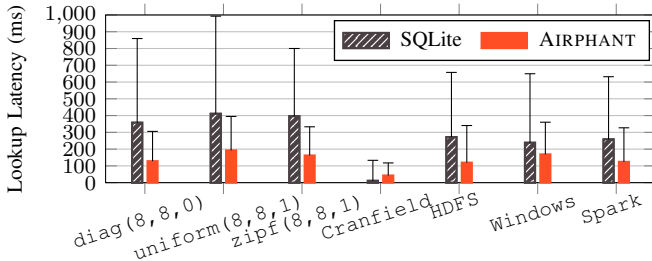


Fig. 14: Term index lookup latencies of indexes on different datasets. Solid bars show average latencies while the upper error bars show 99th percentiles of measured latencies.

($B \geq 1500$) are similar due to stochasticity, higher settings of B generally results in a faster search. It should come as no surprise that spending more resource (memory in this case) results in a better performance.

The number of layers L has the most impact on the storage usage because it roughly determines how many bins each posting would belong to. In the worst case where no common postings fall into the same bin, the storage usage is a linear function of L ; however, Figure 16d reveals a sublinear relationship, especially in small B . This is due to a high chance of word's hash collision, inducing more intersection of postings. Developing a hash function that promotes such

intersection to save space while controlling false positives is a promising future direction. Moreover, L also approximately linearly affects term lookup latencies as presented in Figure 16c. Thanks to concurrent network communication, lookup latency is substantially smaller than a multiple of L ; for example, lookup latency for $L = 16$ is much less than $16 \times$ of that for $L = 1$.

D. Tighter Accuracy Requirement

We also study the relationship between expected false positive parameter F_0 on optimal number of layers, and ultimately, search and term index lookup latencies. We select $F_0 \in \{1.0, 0.01, 0.0001\}$ using $B = 10^5$ bins. Then, we observe the optimal numbers of layers L^* , search latency, and term index lookup latency. Despite differences in magnitude from these setting, the resulting optimal number of layers L^* increases only slightly (Figure 17a). This is consistent with but even stronger (in terms of exponentiation base) than the earlier upper bound analysis that the expected number of false positives is exponentially decreasing at $O(2^{-L})$. As we have seen earlier, a small difference in number of layers with fixed number of bins reflects in a slight difference in both search and term index lookup latencies. Overall, Figure 17b displays slight increases in latencies when accuracy parameter increases. Those observations that do not follow the trend do so because of variability in cloud storage.

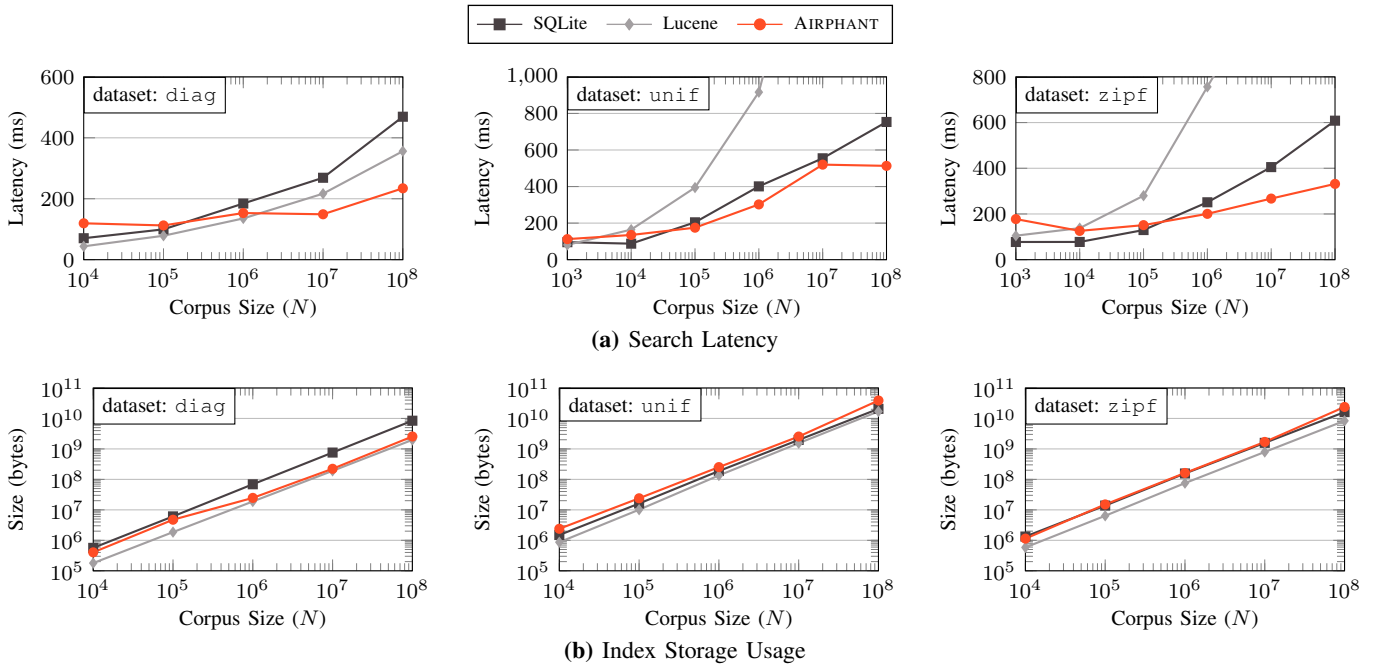


Fig. 15: Effects of corpus size on avg search latency (top) and index size (bottom). Given a corpus size X , synthetic datasets are generated with the numbers of documents and words $n_d = n_w = N = 10^x$: $\text{diag}(x, x, 0)$, $\text{unif}(x, x, 1)$, and $\text{zipf}(x, x, 1)$.

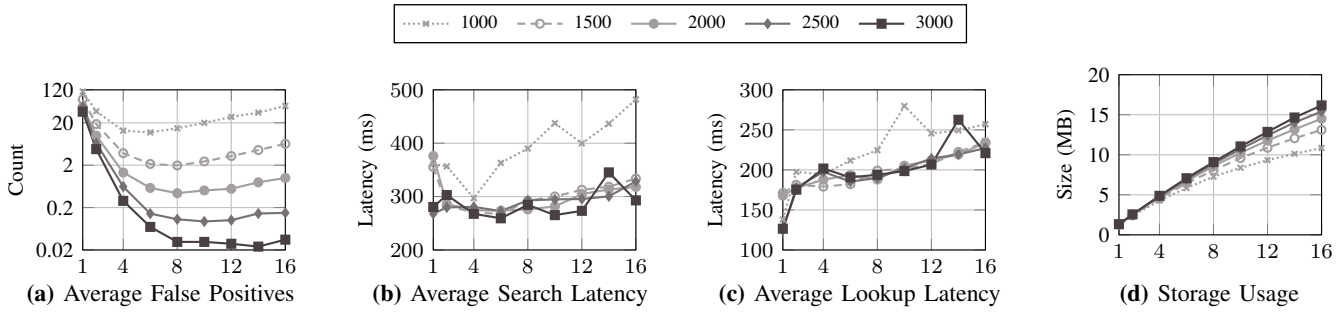


Fig. 16: Effects of numbers of bins B and layers L on average number of false positives, average search latency, average term lookup latency, and index storage size, from left to right. Each line corresponds to a number of bins $B \in \{1000, 1500, \dots, 3000\}$, while x-axis corresponds to the number of layers L . We use Cranfield as the corpus in these experiments.

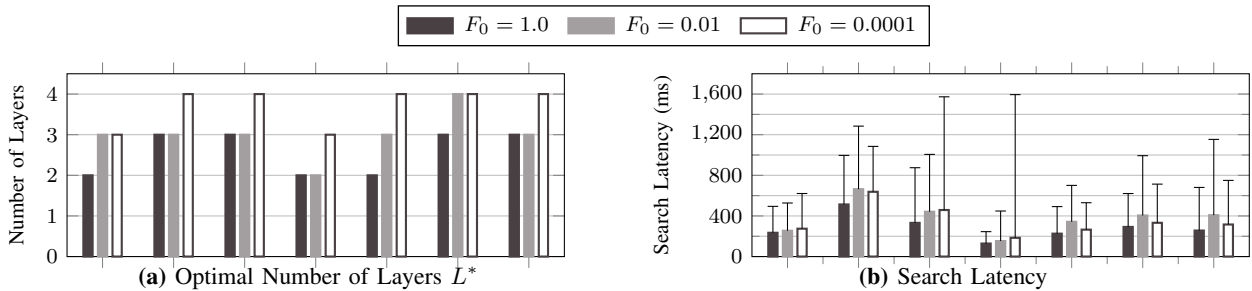


Fig. 17: Latencies of AIRPHANT with different accuracy constraint configurations. Solid bars show average latencies while the upper error bars show 99th percentiles of measured latencies.